sustainability

MDPI

Article

Experimental Research on a Lightweight Miniature Wankel Compressor for a Vapor Compression Refrigeration System in Aerospace

Ruiping Zhi [1,2], Rui Ma [3], Delou Zhang [4] and Yuting Wu [1,2,*]

[1] MOE Key Laboratory of Enhanced Heat Transfer and Energy Conservation, College of Environmental and Energy Engineering, Beijing University of Technology, Beijing 100124, China
[2] Beijing Key Laboratory of Heat Transfer and Energy Conversion, College of Environmental and Energy Engineering, Beijing University of Technology, Beijing 100124, China
[3] Key Laboratory of Wind Energy and Solar Energy Technology, College of Energy and Power Engineering, Inner Mongolia University of Technology, Hohhot 010051, China
[4] China Institute of Atomic Energy, Beijing 102488, China
* Correspondence: wuyuting@bjut.edu.cn; Tel.: +86-10-6739-6662 or +86-156-0051-6677; Fax: +86-10-6739-2774

Abstract: Vapor compression refrigeration is considered one promising technology for dissipating much higher heat fluxes from electronic devices at lower temperatures. The compressor, one key component, has a great effect on the overall size and performance of the system. One lightweight, miniature, hermetic Wankel compressor was developed to solve limited space cooling problems. The assembled Wankel compressor had a diameter of 65 mm, a length of 85 mm and a weight of 340.2 g, without a motor and housing. An experimental system for miniature refrigeration was set up to explore the optimal refrigerant charge and the performance of the compressor under changing rotational speeds and inlet temperatures of cooling water. The experimental results showed that the optimal refrigerant charge was 220 g and the coefficient of performance was approximately 2.8. The refrigeration coefficient of the system decreased with increases in rotational speed and inlet temperature of the cooling water at a stable cooling capacity of 100 W. The developed lightweight, miniature, hermetic Wankel compressor had reliable performance after running for 600 h, with a power consumption of 35 W and a high coefficient of performance (COP) of 2.63.

Keywords: vapor compression refrigeration; aerospace; Wankel compressor; electronics cooling; miniature compressor

Citation: Zhi, R.; Ma, R.; Zhang, D.; Wu, Y. Experimental Research on a Lightweight Miniature Wankel Compressor for a Vapor Compression Refrigeration System in Aerospace. *Sustainability* **2023**, *15*, 8826. https://doi.org/10.3390/su15118826

Academic Editors: Kian Jon Chua and Reza Daneshazarian

Received: 6 March 2023
Revised: 27 April 2023
Accepted: 26 May 2023
Published: 30 May 2023

1. Introduction

In aerospace, thermal control is used to maintain a proper temperature on vehicle surfaces and their components under the multi-task stage of changing thermal loads and ambient temperatures. In order to provide more functions and computing power, the size of spacecraft has increased. However, heat dissipation from electronic equipment and scientific instruments has become a challenge for the design of portable and electronic equipment with limited space. Problems of high heat flux density, large heat transmission and dissipation of spaceborne high-power electronic equipment and devices are increasingly prominent. Liang et al. [1] evaluated three technologies for electronic cooling (heat pipe, thermoelectric and vapor compression refrigeration (VCR) systems) and concluded that VCR is capable of dissipating much higher heat fluxes at lower temperatures than all other technologies. Trutassanawin et al. [2] reviewed different technologies for high heat removal and similarly suggested that VCR can achieve high heat flux. Thus, VCR is one promising technology for cooling electronics and science instruments due to its distinguishing features, including high coefficient of performance (COP), low mass flow rate, low cold plate temperatures and heat removal from source. However, the weight and size of components in VCR systems restrict their application in electronics cooling [3].

The miniature VCR system mainly includes a compressor, condenser, expansion valve and evaporator. The compressor in the cycle is utilized for lifting condenser temperature, reducing the necessary radiator surface area and broadening the thermal control range. Thus, the compressor is one key component that can have a great effect on the overall size and performance of the VCR system, as described by Jeong et al. [4], Trutassanawin et al. [5] and Davies et al. [6].

Many studies have investigated the miniature compressor in the miniature VCR system used in electronic cooling. Trutassanawin et al. [7] carried out experiments on the miniature VCR system for electronics cooling using two different commercially available compressors (a rotary compressor that was 85 mm in diameter, 166 mm in length and 2.8 kg in weight and a reciprocating compressor that was 195 mm in diameter, 204 mm in length and 4.3 kg in weight). The experimental results showed that the cooling COP of the VCR system integrated with the rotary compressor was better than that of the reciprocating compressor because the efficiency of the rotary compressor was greater than that of the reciprocating compressor. It was concluded that the size, efficiency and reliability of the compressor must be considered carefully if a miniature VCR system is to be utilized in electronics cooling. Sathe et al. [8] investigated the performance of a rolling-piston rotary compressor (78 mm in height, 56 mm in diameter and 0.6 kg in weight) manufactured by Aspen Compressor, LLC., Somerset, Kentucky. The system COP ranged from 2.1 to 7.4 at pressure ratios of 2.0 to 3.5. Compared to the experimental results tested by Trutassanawin et al. [7], the Aspen rotary compressor provided better system performance. It was clearly demonstrated that the compressor, with its small size and light weight, has the potential to be used in the miniature VCR system for electronics cooling. Wu et al. [9] experimentally studied the performance of a miniature VCR system using an Aspen rotary compressor (78 mm in height and 58 mm in diameter) under different refrigerant charges. The overall size of the system was $300 \times 230 \times 70$ mm^3 and the system weight was 3.49 kg. The system efficiency varied from 23% to 31% and the main loss was attributed to the compressor. Thus, it was determined that a more efficient compressor of small size and light weight should be the future focus. Sathe et al. [10] investigated the feasibility of electrostatically actuated diaphragm compressors in a miniature VCR system for electronics cooling based on a developed experimentally validated analytical model. However, the complicated fabrication and costs became a serious challenge. Bradshaw et al. [11,12] established a comprehensive model of linear compressors used in electronics cooling and utilized the developed model to explore its energy recovery characteristics compared to those of a reciprocating compressor. The results indicated that the linear compressor was not sensitive to the dead volume and obtained better efficiency than the reciprocating compressor. Liang et al. [13] suggested that the linear compressor has advantages over conventional compressors. However, there is a lack of quantitative analyses of the advantages of linear compressors. Furthermore, control, mass production and cost have become major limitations in miniature VCR applications. Zhang et al. [14,15] established an experimentally validated model of a linear compressor in a VCR system. In the experiments, a commercially linear compressor was used with a piston that was 26.5 mm in diameter and 76.9 mm in length. The weight of the piston, spring and discharge valve was 0.632 kg, 0.164 kg and 4 g, respectively. The results of the model showed that frequency plays an important role in the performance of linear compressors. Heppner et al. [16] designed a Wankel compressor for a miniature VCR system (367 mm^3 in displacement, 25 mm $\times$ 30 mm in footprint and 6.25 mm in thickness). The system was designed with a cooling capacity of 45 W at 1000 rpm and R134a was used as the working fluid. The system COP could be theoretically achieved at 4.6. Zhang et al. [17] presented a simulation model of a memo-scale Wankel compressor and investigated the effect of friction loss and leakage on its performance based on this model. Wu et al. [18] designed two open-type miniature Wankel compressors without any air outlet valves. The first-generation compressor was fabricated from cast iron and its weight was 0.7 kg. The second-generation compressor was fabricated from high-Si aluminum alloys and its weight was 0.4 kg (50 mm in diameter and 70 mm in height). The experiments carried out on

the second-generation compressor showed that its cooling capacity was above 300 W and the system COP was approximately 2.3. However, the leakage of the open-type Wankel compressor was not good after much use.

In most projects, cooling capacity is normally required to be greater than or equal to 100 W and the compressor weight should be less than 0.5 kg. Thus, the weight and sealing of the Wankel compressor must be further optimized to solve the problems of high heat flux density, large heat transmission and dissipation of spaceborne high-power electronic equipment and devices. In this paper, seeking a more compact and portable device, the lightweight version of the Wankel compressor is investigated in relation to its sealing, housing, and materials. To reduce the possibility of leakage, a hermetic Wankel compressor was developed. Its experimental set-up using R134a was designed to explore the influence of refrigerant charge, rotational speed and inlet temperature of the cooling water on the performance of a lightweight Wankel compressor.

2. Development of a Lightweight Miniature Wankel Compressor

Based on the comprehensive thermal control conditions and design requirements, the parameters of the Wankel compressor were determined as represented in Table 1.

Table 1. The parameters of the Wankel compressor.

Item	Parameter	Item	Parameter
Rated voltage	DC 24 V	Continuous running time	≥5000 h
Current	1–5 A	Cooling capacity	≥100 W
Weight	≤500 g	Maximum compression ratio	3.5
Maximum exhaust temperature	130 °C		

As listed in Table 1, the weight of the Wankel compressor, without accounting for the motor and housing, was less than 500 g. In this paper, two approaches were adopted to achieve the light weight. One way was to optimize the structure of the Wankel compressor, such as removing redundant parts of the component and designing new structures. The other was to optimize the material by using low-density materials instead of steel to reduce the weight.

2.1. The Structure Design

Based on the two generations of open-type miniature Wankel compressors designed in [18], the structural design was optimized in terms of sealing and housing. The sealing method of the Wankel compressor was changed from open type to hermetic type. The DC brushless motor and compressor were enclosed in the housing and connected by a common shaft. Compared to the previous compressor, the front cover, coupling and shaft seals were eliminated. As a result, the overall weight and size of the compressor were reduced. At the same time, the possibility of leakage of the refrigerant and lubricating oil was also reduced.

According to the relevant design standards of the pressure vessel and the internal pressure of the shell, the thickness of the shell was calculated and checked. The housing was changed from three segments to two segments, and its wall thickness was decreased from 8 mm to 4 mm. Axial suction, instead of radial suction, was selected as the compressor suction way.

2.2. The Parts Material

In order to further reduce the weight of the parts, the material optimization design was carried out based on structural optimization. According to the performance requirements of the compressor and the physical properties of the materials, materials with a low density such as titanium alloy, cast aluminum alloy ZL305A and aluminum alloy 7075 were selected. The density of the aluminum alloy was lower than that of the titanium alloy, and the cutting performance and cost of the aluminum alloy were better than those of the titanium alloy.

In this paper, aluminum alloy 7075 was selected as the material for compressor parts such as the front cover, cylinder, back cover and external back cover (presented in Figure 1). The friction surfaces of the above parts adopted the laser cladding technique to satisfy wear resistance requirements.

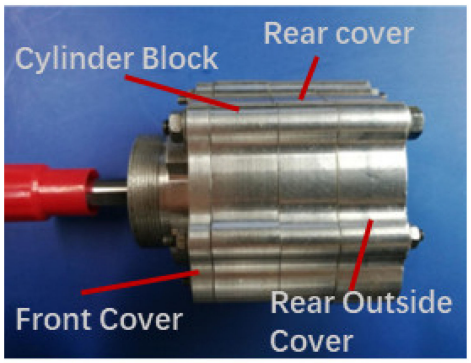

Figure 1. The assembled Wankel compressor.

Because the eccentric shaft and triangular rotor were the main moving parts of the compressor, Ni-Cr alloy cast iron was still used to ensure that the eccentric shaft and triangular rotor had sufficient strength and stiffness in the working process. The weight of each part was tested before and after the weight was reduced, and the comparison is listed in Table 2. The compressor assembled by the above parts weighed 340.2 g with a diameter of 65 mm and a length of 85 mm, as displayed in Figure 1. The weight satisfied the design requirements.

Table 2. Comparison of parts weight of the compressor.

Part	Pre-Optimization Quality/g	Optimized Quality/g	Amount of Change/g
Eccentric shaft	39.3	39.3	0
Triangular rotor	46.1	46.1	0
Cylinder	142.6	61.4	−81.2
Front cover	137.0	59.0	−78.0
Back cover	146.5	63.1	−83.4
Rear outer cover	71.2	71.2	0

2.3. Motor Selection

According to the requirements of compressor torque design, a series of matching and test works were carried out for the motor, as represented in Figure 2. The B3630 brushless motor was an in-runner motor that had the characteristics of high precision, small size, light weight and long service life. Thus, it was suitable for the lightweight requirements of a miniature Wankel Compressor. At first, the motor was not enclosed in the housing with the compressor. There was some leakage of refrigerant and lubricating oil during the performance experiment. In order to reduce the possibility of leakage, the DC brushless motor presented in Figure 2 and the compressor were enclosed in the housing. However, when the condensation temperature was 40 °C and the evaporation temperature was 8~12 °C, the torque of the DC brushless motor was far less than that required by the compressor, which made the compressor unable to work normally.

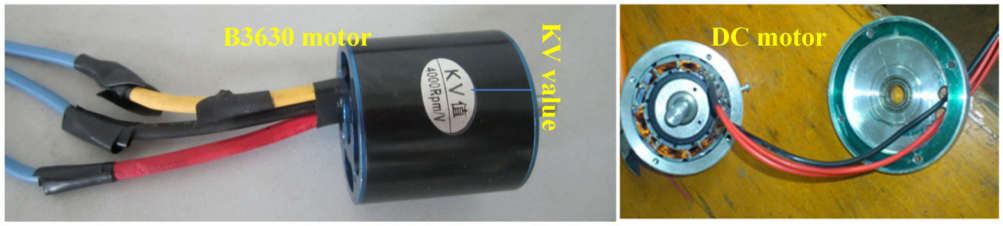

Figure 2. Brushless motor.

The torque required by the normal operation of the Wankel compressor was calculated to be 0.4~0.5 N·m. Therefore, the large torque motor as given in Figure 3 was selected and connected to the Wankel compressor via coupling with an open-type Wankel compressor. The performance test of the compressor showed that the compressor could meet the requirement of 100 W cooling capacity, but it was too heavy to meet the weight requirements.

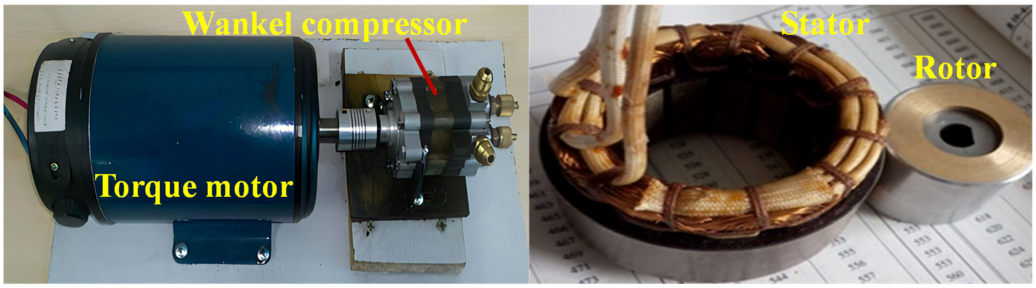

Figure 3. Torque motor.

According to the weight requirements, the DC torque motor with a locked rotor torque of 0.433 N·m and 1500 rpm was manufactured by our commission and shared the common shaft with the Wankel compressor. The Wankel compressor and the DC torque motor were enclosed in the housing. The performance test showed that when the refrigerating capacity of the compressor reached 100 W, the condensing temperature was 18 °C, the operating voltage of the compressor was 24 V, the current was 1.4 A and the COP of the system was 2.98. However, the maximum pressure ratio was just 1.5.

It can be observed from the analysis that the low rotational speed of the motor was the main reason for the small compression ratio. According to the requirements for the compression ratio and torque of the compressor, combined with the lightweight scheme and the above motor-matching process, the Beijing Shuguang motor factory was entrusted to develop a DC brushless motor with a torque of 0.433 N·m and a maximum speed of 10,000 rpm. The stator and rotor of the motor are represented in Figure 3. The motor was connected to the Wankel compressor by a common shaft without coupling and the motor and compressor were enclosed in the housing together.

2.4. Lightweight Compressor Development

During the development process of the lightweight Wankel compressor, three generations of the device were designed and developed. For the first generation, all parts of the compressor were made of Ni-Cr alloy cast iron. The compressor was connected to a DC brushless motor by coupling. The housing material was 45 steel with a thickness of 8 mm. For the second generation, the compressor parts were made of Ni-Cr alloy cast iron. The compressor and DC brushless motor were connected by a common shaft. The housing material was 45 steel with a thickness of 4 mm. For the third generation, the parts of the compressor were made of aluminum alloy 7075. The compressor and DC brushless motor were connected by a common shaft. The housing material was duralumin with a thickness of 4 mm. The indicators of each generation of the lightweight compressor are observed in Table 3 and the prototypes are represented in Figure 4.

Table 3. The development process of the Wankel compressor.

Item	First	Second	Third
Housing material	45 steel	45 steel	duralumin
Housing thickness	8 mm	4 mm	4 mm
Coupling	yes	yes	no
Compressor weight	3.925 kg	2.855 kg	1.490 kg
Compressor length	240 mm	190 mm	155 mm

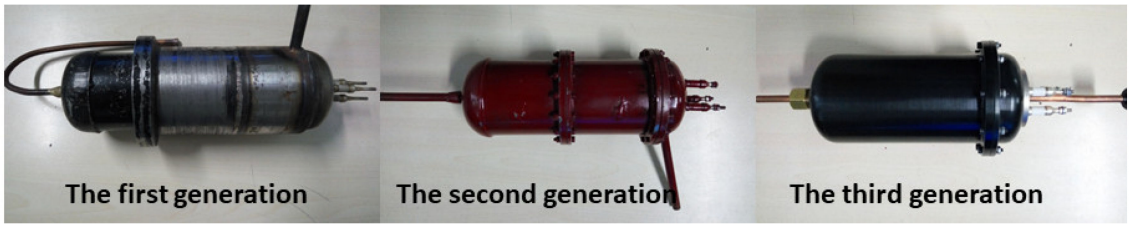

Figure 4. The prototypes of the Wankel compressor.

3. Performance Experiment and Analysis

3.1. Experimental System

The refrigeration performance of the developed lightweight, miniature Wankel compressor was tested. The refrigeration system of the lightweight, miniature Wankel compressor was composed of a lightweight, miniature Wankel compressor, compact condenser (plate heat exchanger), sight glass, drying filter, compact evaporator and capillaries, as observed in Figures 5 and 6. The water cycle system was an auxiliary system to provide constant temperature conditions for the condenser in the refrigeration system. It mainly included a water pump, mass flowmeter, regulator valve and constant temperature water baths. The main parameters of the components used in the experimental setup are presented in Table 4.

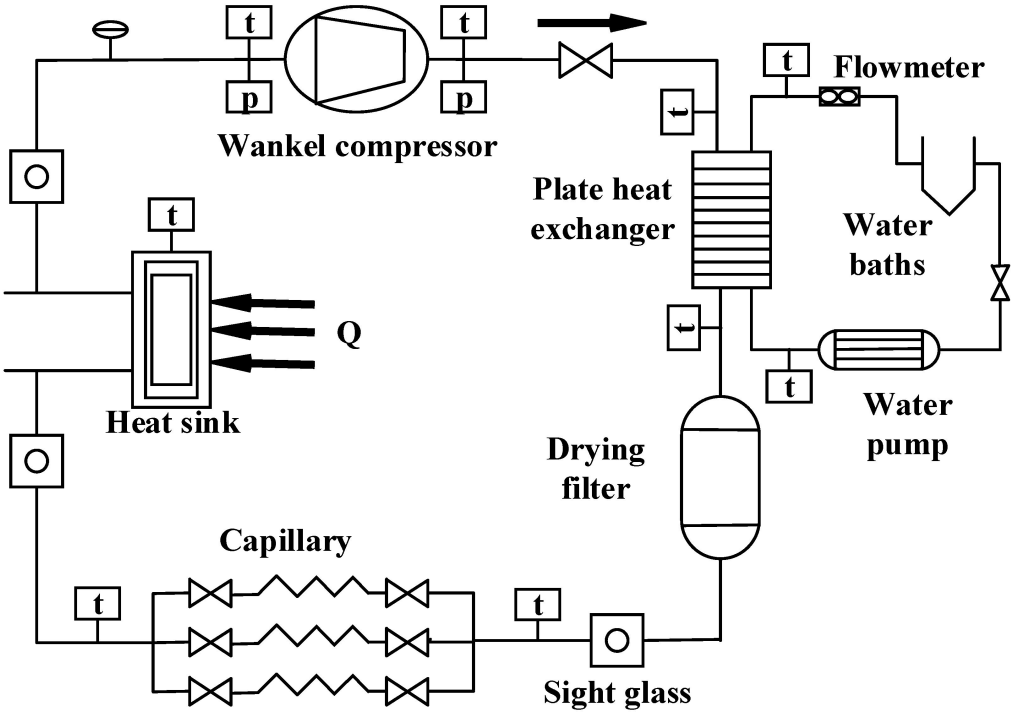

Figure 5. A schematic diagram of the experimental system for testing the miniature cooling system.

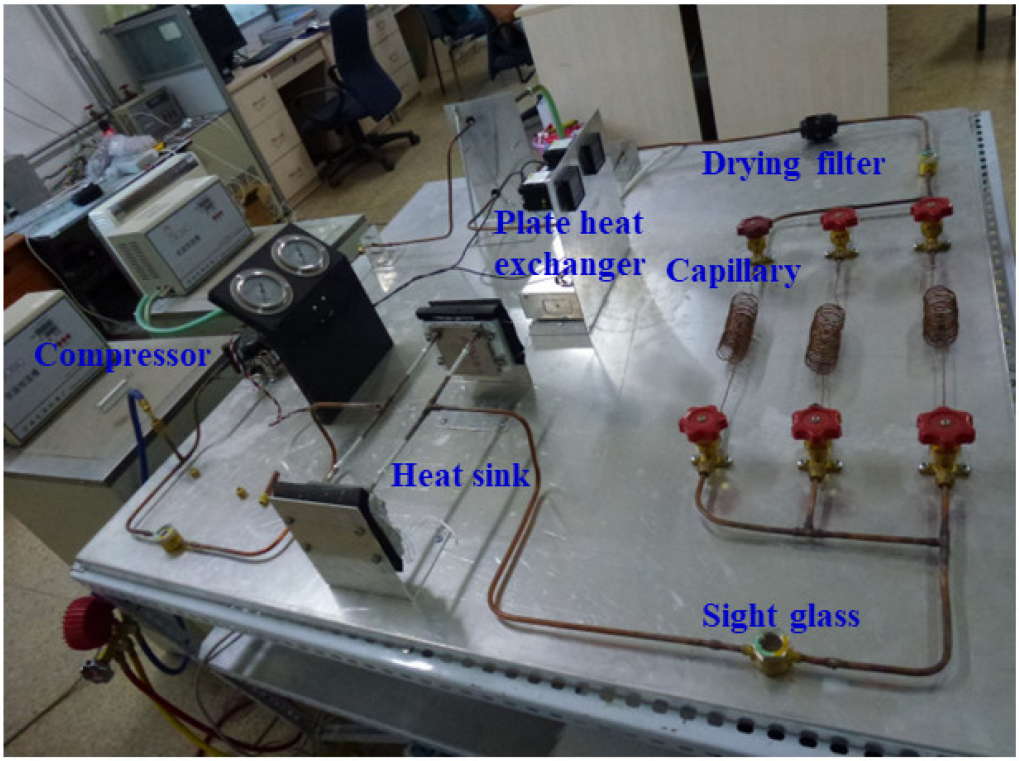

Figure 6. Photo of the experimental system for testing the miniature cooling system.

Table 4. Main parameters of the components.

Components	Parameters
Heat sink	Channel width: 2 mm; Overall pressure drop: 1.68×10^4 Pa Heat exchange length: 0.777 m
Compressor	Generating radius: 18 mm; Eccentricity: 3 mm
Plate heat exchanger	Type: Brazed plate type; Heat transfer coefficient: 2500 W/m^2·K Pressure Range: 3.0 MPa; Temperature range: −160~300 °C
Capillary	Material: Red copper; Inside diameter: 0.64 × 1 mm; Calculated length: 2.75 m

In the experiment, the refrigerant was R134a. The lubricant and refrigerant were circulated without separation for microgravity adaptation. In the microgravity environment, the refrigerant and lubricating oil needed to be uniformly mixed. Hence, it was better to ensure the long-term stable operation of the compressor. Thus, the lubricant SUNISO SL-32S (VG32) was selected because it has good compatibility with the refrigerant R134a. The micro-channel phase change heat exchanger was used as the evaporator and the electric heating film on its wall provided a constant heat load of 100 W through the aluminum block. The brazed plate heat exchanger was selected as the condenser and its working temperature ranged from −160 to 300 °C. Temperatures were measured with PT100 thermocouples with ±0.15 °C accuracy. All pressures were measured with pressure transducers that had an accuracy of ±0.25%. The uncertainties of temperature, pressure and COP were 1.7%, 2.7% and 7.1%, respectively. A refrigeration performance test was carried out to find out the optimal operating conditions of the system by changing the refrigerant charge, compressor speed and cooling water temperature.

3.2. Influence of Refrigerant Charge on Compressor Performance

3.2.1. Evaporation Pressure and Condensation Pressure

Figure 7 presents the variation of condensation and evaporation pressure/temperature with different refrigerant charges. With an increase in refrigerant charge, the evaporation pressure greatly increased from 5.7 bar to 6.2 bar. The condensation pressure only increased slightly and kept almost constant at approximately 7.7 bar. When the refrigerant charge was appropriate, the refrigerant fully soaked the heat exchange surface in the evaporator, with a good heat exchange effect and appropriate evaporation. The growth of the refrigerant charge led to an increase in heat exchange in the evaporator and in the evaporation capacity, which resulted in an increase in evaporation pressure. The suction-specific volume generally decreased with an increase in evaporation pressure. Hence, the mass flow rate of the refrigerant and the displacement of the compressor increased. As a result, the refrigerant in the condenser grew and the condensation pressure increased. Therefore, during the charging process, an excessive refrigerant charge needed to be avoided because this could lead to a large amount of liquid refrigerant accumulating in the evaporator and condenser. This could cause an increase in evaporation pressure and temperature, suction pressure of the compressor, and condenser temperature and pressure. It could also cause the liquid refrigerant or refrigerant droplets that were not fully evaporated to flow into the compressor, which could result in the phenomenon of a "liquid attack" in the compressor. With an increase in refrigerant charge, the evaporation temperature showed a rapidly rising trend from 20.3 °C to 22.7 °C and the condensation temperature of the system kept almost constant at approximately 30 °C, which was consistent with the changing trend of evaporation pressure and condensation pressure.

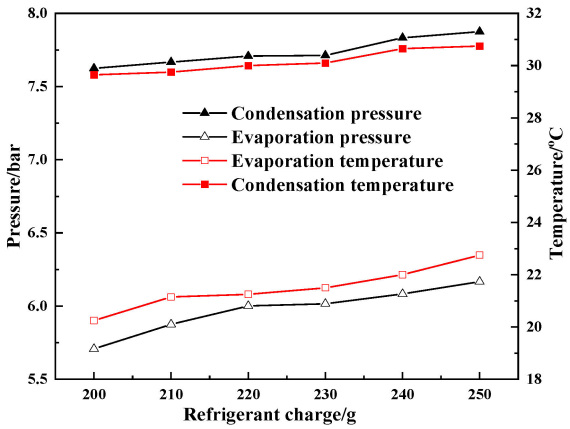

Figure 7. Evaporation and condensation pressure/temperature with different refrigerant charges.

3.2.2. Compressor Power Consumption

Figure 8 describes the variation of the power consumption of the compressor against refrigerant charge at a constant cooling capacity of 100 W. As the refrigerant charge increased, the power consumption of the compressor first decreased and then increased. A minimum power consumption of 40 W was achieved at a refrigerant charge of approximately 220 g. When the refrigerant charge in the system was higher than the optimal charge, the refrigerant in the condenser accumulated and the effective surface participating in the heat transfer decreased. With an increase in condensation temperature and pressure, the compressor energy consumption increased.

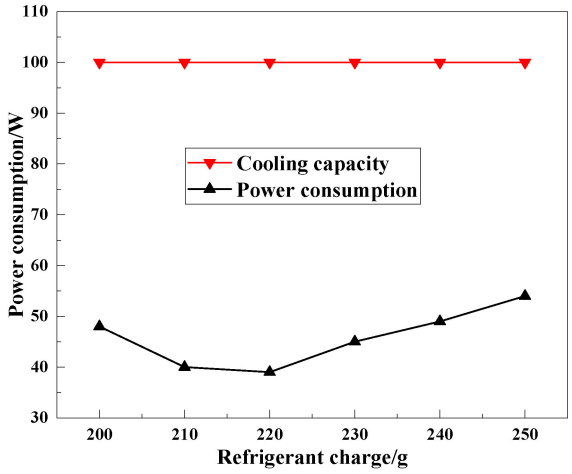

Figure 8. Power consumption of the compressor with refrigerant charge.

3.2.3. COP

It can be observed from Figure 9 that when the cooling capacity (heat load of the evaporator) was 100 W, the optimal refrigerant charge range of the micro refrigeration system was 210–220 g. A refrigerant charge that was not enough or too much was not good for the operation of the compressor or refrigeration system. When the refrigerant charge was not enough and the evaporator refrigerant amount was not fully filled, the evaporation pressure decreased and the suction superheat of the compressor increased so that the heat transfer coefficient and refrigeration capacity were reduced. Too much refrigerant charge reduced the cooling capacity and increased the power consumption, and the heat transfer coefficient declined faster than that in the case of an inadequate refrigerant charge.

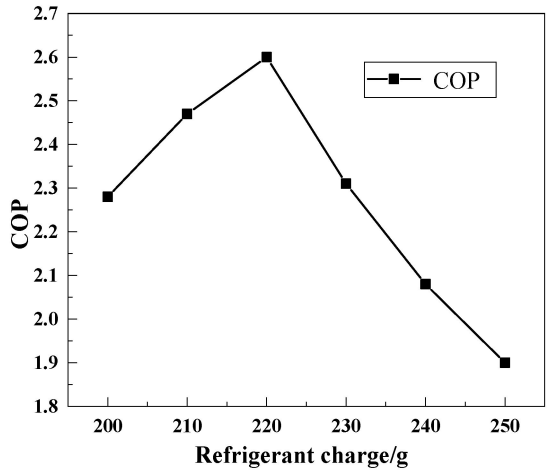

Figure 9. COP with refrigerant charge.

3.3. Influence of Rotational Speed on Compressor Performance

3.3.1. Suction and Discharge Temperature and Pressure of Compressor

Figure 10 displays the changes in suction temperature, discharge temperature, suction pressure and discharge pressure with different rotational speeds. With an increase in rotational speed, the suction pressure and temperature of the compressor decreased slightly, while the discharge temperature and pressure of the compressor increased greatly from 30.2 °C to 51.2 °C and from 7.7 bar to 14.3 bar, respectively. When the rotational speed was at 4800 rpm, the suction pressure and discharge pressure were 5.1 bar and 14.3 bar, respectively, and the compressor COP reached approximately 2.8. Because the rotational

speed increased, the mass flow rate of the refrigerant increased, which lead to a slight decrease in the evaporation pressure, a clear increase in discharge pressure and temperature, and an increase in the compression ratio.

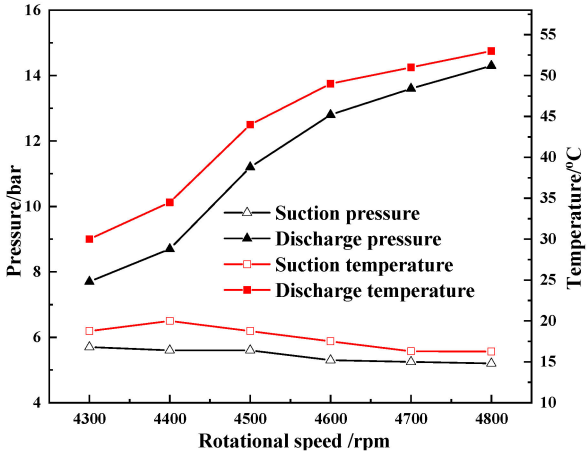

Figure 10. The suction and discharge pressure/temperature with rotational speed.

3.3.2. Compressor Power Consumption

According to Figure 11, the power consumption of the compressor increased with an increase in rotational speed. This is because an increase in rotational speed led to an increase in the mass flow rate of the refrigerant and the pipe resistance.

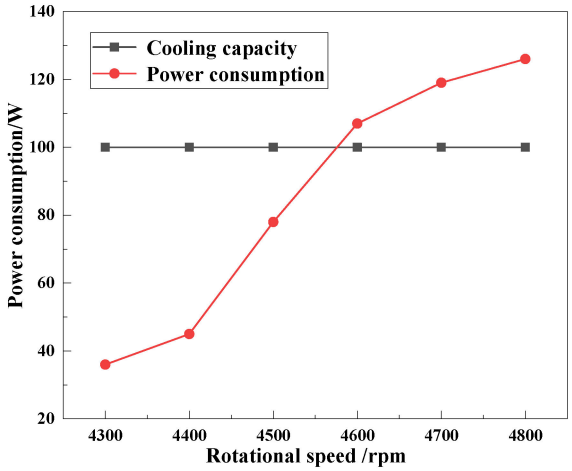

Figure 11. The power consumption with rotational speed.

3.3.3. COP

Figure 12 presents the effect of the rotational speed of the Wankel compressor on the COP. The COP decreased rapidly at first and then slowly with an increase in rotational speed. This was due to the increase in the power consumption of the compressor with the increase in rotational speed, while the cooling capacity remained stable at 100 W. Considering the power consumption, COP and cooling capacity, the higher rotational speed of the compressor was not good for improving system performance. Therefore, the rotational speed of the compressor was too high.

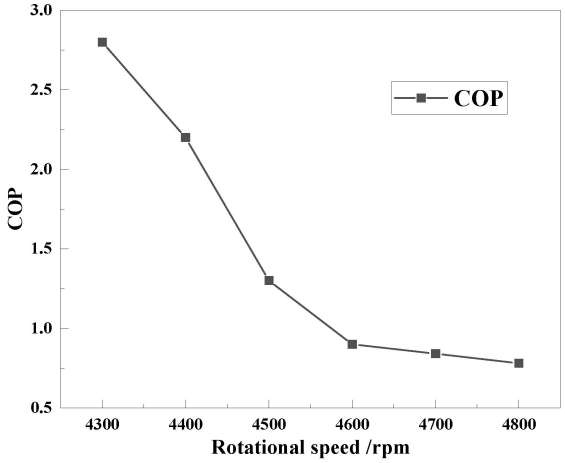

Figure 12. The COP with rotational speed.

3.4. The Effect of Cooling Water Temperature on Compressor Performance

3.4.1. Suction and Discharge Temperature of the Compressor

Figure 13 presents the variation in the suction and discharge temperature of the compressor with different inlet temperatures of cooling water. Figure 13 also presents the change in the suction and discharge pressure of the compressor with different inlet temperatures of cooling water. From Figure 12, it can be observed that when the inlet temperature of the cooling water changed from 25 °C to 45 °C, the suction temperature and suction pressure increased slightly, while the discharge temperature and discharge pressure increased greatly.

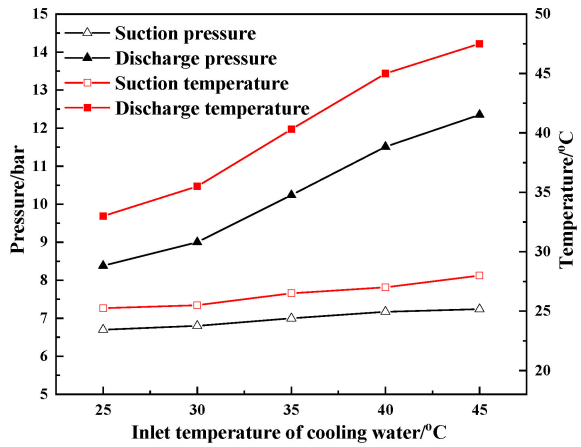

Figure 13. The suction and discharge pressure/temperature with the inlet temperature of the cooling water.

3.4.2. Compressor Power Consumption

From Figure 14, it can be observed that the power consumption of the Wankel compressor increased rapidly from 26 W to 103.6 W when the inlet temperature of the cooling water on the condenser side rose from 25 °C to 45 °C. This is because an increase in the inlet temperature of cooling water led to an increase in the condensation pressure and evaporation pressure, and the increase in condensation temperature was greater than that for the evaporation temperature. Hence, the compression ratio increased, which caused an increase in power consumption.

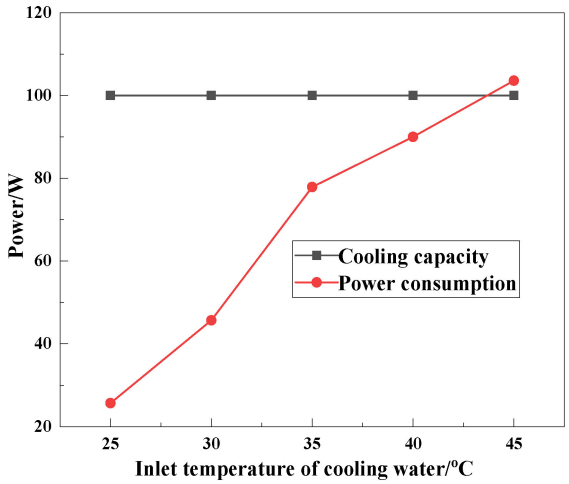

Figure 14. The power consumption with inlet temperature of the cooling water.

3.4.3. COP

Figure 15 reveals that the COP decreased from 3.2 to 0.98 with an increase in the inlet temperature of the cooling water. As the inlet temperature of the cooling water increased, the power consumption rose rapidly. However, the refrigeration capacity remained constant. Thus, the COP decreased dramatically from 3.2 to 0.98. As a result, to improve the COP, the inlet temperature of the cooling water should not be too high.

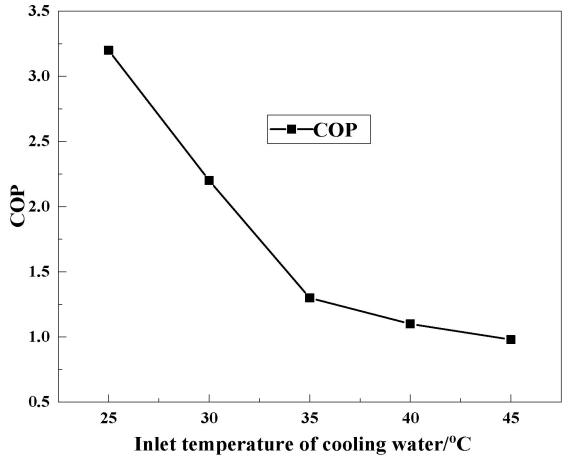

Figure 15. The COP with inlet temperature of the cooling water.

3.5. Reliability Life Test

The purpose of the reliability life test is to understand the life characteristics, failure law, average life and possible failure modes in the process of life. It can be divided into two tests: the working life test and the storage life test. The compressor was designed for cooling electronic devices in the aerospace field. Thus, it was of great importance to conduct a reliability life test for the system.

The reliability life test bench of the Wankel compressor was established. In the experiment, the refrigeration load of the evaporator was set to 100 W, the rotational speed of the motor was controlled at approximately 4400 rpm, the inlet temperature of the cooling water was 30 °C and the mass flow rate of cooling water was 35 kg/h. The temperature variation of the heat sink with time is displayed in Figure 16. In the experiment, the heat sink was first heated by the power supply and its temperature increased to approximately 42 °C. Then, the compressor started and the refrigeration system began working. The temperature of the heat sink rapidly decreased to approximately 26 °C after running the refrigeration system.

Next, the temperature of the heat sink remained stable after continuing the refrigeration system. After normal operation for 600 h, the power consumption of the compressor was 38 W and the system COP was 2.63.

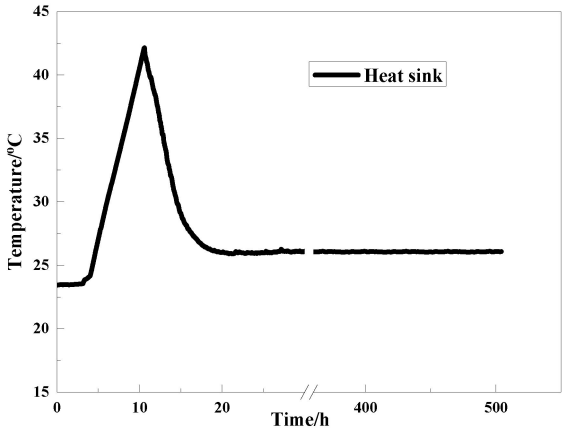

Figure 16. The heat sink temperature.

4. Conclusions

Based on the miniature refrigeration system for space, a lightweight, miniature, hermetic Wankel compressor was developed. An experimental system for the miniature cooling system was established with a heat load of 100 W for the evaporator, and the effects of refrigerant charge, rotational speed of the compressor and inlet temperature of the cooling water on the refrigeration performance of the compressor were investigated. The following conclusions can be drawn:

(1) According to the working principle of the Wankel compressor and the requirements of the miniature refrigeration system, research on a lightweight, miniature, hermetic Wankel compressor has been carried out. The assembled compressor, without housing and motor, had a diameter of 65 mm, height of 85 mm and weight of 340.2 g.
(2) The optimal refrigerant charge of the system was 220 g under a cooling capacity of 100 W. The minimum power consumption was achieved at approximately 40 W and the maximum COP was 2.5.
(3) When the rotational speed was at 4300 rpm, the power consumption was 35 W and the maximum COP was 2.8. An increase in the rotational speed led to a decrease in the evaporation temperature and COP. When the rotational speed increased from 4300 rpm to 4800 rpm, the COP dropped sharply from 2.8 to 0.8.
(4) When the inlet temperature of the cooling water was 25 °C, the maximum COP was obtained at approximately 3.2. To improve the COP, the inlet temperature of the cooling water should not be too high.
(5) The reliability life test was carried out for 600 h. This reliability life test proved the reliability of the Wankel compressor.
(6) The compressor was developed to solve the problem of high heat dissipation in spacecraft. Compressor performance optimization under the microgravity and high vacuum environment shall be the focus of future research.

Author Contributions: Conceptualization, R.Z., R.M., D.Z. and Y.W. All authors have read and agreed to the published version of the manuscript.

Funding: This research was funded by [R&D Program of Beijing Municipal Education Commission] grant number [KM202310005016].

Institutional Review Board Statement: Not applicable.

Informed Consent Statement: Not applicable.

Data Availability Statement: The data that support the findings of this study are available from the corresponding author upon reasonable request.

Acknowledgments: The authors are grateful for the financial support provided by R&D Program of Beijing Municipal Education Commission (KM202310005016), the Beijing Municipal Natural Science Foundation (no. 3181001), and the National Science Foundation of China (no. 51906116).

Conflicts of Interest: The authors declare no conflict of interest.

References

1. Liang, K.; Li, Z.; Chen, M.; Jiang, H. Comparisons between heat pipe, thermoelectric system, and vapour compression refrigeration system for electronics cooling. *Appl. Therm. Eng.* **2019**, *146*, 260–267. [CrossRef]
2. Trutassanawin, S.; Groll, E.A. Review of Refrigeration Technologies for High Heat Dissipation Electronics Cooling. In Proceedings of the International Refrigeration and Air Conditioning Conference at Purdue University, West Lafayette, IN, USA, 12–15 July 2004.
3. Possamai, F.; Lilie, D.E.B.; Zimmermannn, A.J.P.; Mongia, R. Miniature Vapor Compression System. In Proceedings of the International Refrigeration and Air Conditioning Conference, West Lafayette, IN, USA, 14–17 July 2008; p. 963.
4. Jeong, S. How difficult is it to make a micro refrigerator? *Int. J. Refrig.* **2004**, *27*, 309–313. [CrossRef]
5. Trutassanawin, S.; Groll, E.A.; Garimella, S.V.; Cremaschi, L. Experimental Investigation of a Miniature-Scale Refrigeration System for Electronics Cooling. *IEEE Trans. Compon. Packag. Technol.* **2006**, *29*, 678–687. [CrossRef]
6. Davies, G.F.; Eames, I.W.; Bailey, P.; Dadd, M.; Janiszewski, A.; Stone, R.; Maidment, G.; Agnew, B. Cooling microprocessors using vapor compression refrigeration. In Proceedings of the 12th IEEE Intersociety Conference on Thermal and Thermomechanical Phenomena in Electronic Systems (ITherm), Las Vegas, NV, USA, 2–5 June 2010; pp. 1–8.
7. Trutassanawin, S. A Miniature-Scale Refrigeration System for Electronics Cooling. Ph.D. Thesis, Purdue University, West Lafayette, IN, USA, 2006.
8. Sathe, A.A.; Groll, E.A.; Garimella, S.V. Experimental evaluation of a miniature rotary compressor for application in electronics cooling. In Proceedings of the International Compressor Engineering Conference, West Lafayette, IN, USA, 14–17 July 2008; p. 1115.
9. Wu, Z.; Du, R. Design and experimental study of a miniature vapor compression refrigeration system for electronics cooling. *Appl. Therm. Eng.* **2011**, *31*, 385–390. [CrossRef]
10. Sathe, A.A.; Groll, E.A.; Garimella, S.V. Optimization of electrostatically actuated miniature compressors for electronics cooling. *Int. J. Refrig.* **2009**, *32*, 1517–1525. [CrossRef]
11. Bradshaw, C.R.; Groll, E.A.; Garimella, S.V. A comprehensive model of a miniature-scale linear compressor for electronics cooling. *Int. J. Refrig.* **2011**, *34*, 63–73. [CrossRef]
12. Bradshaw, C.R.; Groll, E.A.; Garimella, S.V. Linear compressors for electronics cooling: Energy recovery and its benefits. *Int. J. Refrig.* **2013**, *36*, 2007–2013. [CrossRef]
13. Liang, K. A review of linear compressors for refrigeration. *Int. J. Refrig.* **2017**, *84*, 253–273. [CrossRef]
14. Zhang, X.Y.; Ziviani, D.; Braun, J.E.; Groll, E.A. Experimental Validation and Analysis of a Dynamic Model for Linear Compressors. In Proceedings of the 24th International Compressor Engineering Conference at Purdue, West Lafayette, IN, USA, 9–12 July 2018.
15. Zhang, X.Y.; Ziviani, D.; Braun, J.E.; Groll, E.A. Theoretical analysis of dynamic characteristics in linear compressors. *Int. J. Refrig.* **2020**, *109*, 114–127. [CrossRef]
16. Heppner, J.D.; Walther, D.C.; Pisano, A.P. The design of ARCTIC: A rotary compressor thermally insulated µcooler. *Sens. Actuators A Phys.* **2007**, *134*, 47–56. [CrossRef]
17. Zhang, Y.; Wang, W. Effects of leakage and friction on the miniaturization of a Wankel compressor. *Front. Energy* **2011**, *5*, 83–92. [CrossRef]
18. Wu, Y.T.; Ma, C.F.; Zhong, X.H. Development and experimental investigation of a miniature-scale refrigeration system. *Energy Convers. Manag.* **2010**, *51*, 81–88. [CrossRef]